Cerebrospinal Fluid cfDNA Sequencing for Classification of Central Nervous System Glioma

Florian Iser[1], Felix Hinz[2,3], Dirk C. Hoffmann[1,4], Niklas Grassl[5,6], Cansu Güngoör[7], Jochen Meyer[2,3], Laura Dörner[2,3], Lea Hofmann[2,3], Vanessa Kelbch[2,3], Kirsten Göbel[2,3], Mustafa Ahmed Mahmutoglu[8], Philipp Vollmuth[8], Areeba Patel[2,3], Duy Nguyen[9], Leon D. Kaulen[1,7], Iris Mildenberger[5,6], Katharina Sahm[5,6], Kendra Maaß[10,11], Kristian W. Pajtler[10,11], Ganesh M. Shankar[12], Markus Weiler[7], Brigitte Wildemann[13], Frank Winkler[1,14], Andreas von Deimling[2,3], Michael Platten[5,6], Wolfgang Wick[1,14], Felix Sahm[2,3], and Tobias Kessler[1,14]

ABSTRACT

Purpose: Primary central nervous system (CNS) gliomas can be classified by characteristic genetic alterations. In addition to solid tissue obtained via surgery or biopsy, cell-free DNA (cfDNA) from cerebrospinal fluid (CSF) is an alternative source of material for genomic analyses.

Experimental Design: We performed targeted next-generation sequencing of CSF cfDNA in a representative cohort of 85 patients presenting at two neurooncological centers with suspicion of primary or recurrent glioma. Copy-number variation (CNV) profiles, single-nucleotide variants (SNV), and small insertions/deletions (indel) were combined into a molecular-guided tumor classification. Comparison with the solid tumor was performed for 38 cases with matching solid tissue available.

Results: Cases were stratified into four groups: glioblastoma ($n = 32$), other glioma ($n = 19$), nonmalignant ($n = 17$), and nondiagnostic ($n = 17$). We introduced a molecular-guided tumor classification, which enabled identification of tumor entities and/or cancer-specific alterations in 75.0% ($n = 24$) of glioblastoma and 52.6% ($n = 10$) of other glioma cases. The overlap between CSF and matching solid tissue was highest for CNVs (26%–48%) and SNVs at predefined gene loci (44%), followed by SNVs/indels identified via uninformed variant calling (8%–14%). A molecular-guided tumor classification was possible for 23.5% ($n = 4$) of nondiagnostic cases.

Conclusions: We developed a targeted sequencing workflow for CSF cfDNA as well as a strategy for interpretation and reporting of sequencing results based on a molecular-guided tumor classification in glioma.

See related commentary by Abdullah, p. 2860

Introduction

Central nervous system (CNS) tumors still harbor a high mortality rate (1). For patients with glioblastoma, the median overall survival remains at around 15 months despite optimal multimodal therapy (2). Defining the optimal treatment of CNS tumors relies on identification of the correct tumor subtype. This diagnosis is based on the analysis of tumor tissue. Recent advances in molecular profiling of CNS tumors established molecular markers including *IDH* and 1p/19q to be mandatory for the diagnosis of gliomas (3).

However, sampling tumor tissue for diagnostic purposes could carry a potential risk depending on the anatomic location. In addition, patients with recurrent or progressive tumors may not wish to undergo *de novo* biopsy to track tumor evolution in search for new therapy targets, defining the need for minimally invasive liquid biopsies to identify molecular tumor characteristics.

Already today, blood-based liquid biopsies are used in routine cancer diagnostics and progression monitoring of extracerebral tumors (4, 5). However, circulating tumor DNA (ctDNA) is found in the blood of less than 10% of patients with glioma and the blood–brain barrier is suspected to prevent glioma ctDNA from entering the bloodstream (6). Sequencing of cell-free DNA (cfDNA) from cerebrospinal fluid (CSF) has been established as a method to detect tumor mutations and copy-number variations (CNV) in brain tumors with minimal invasiveness (7). Specific diagnosis guiding mutations such as H3.3 K27M mutations in diffuse midline glioma (DMG) have been discovered with reliable follow-up possibilities (8). In pediatric populations, recent studies made advances in classification of brain tumors based on specific mutations found in the CSF (9).

[1]Clinical Cooperation Unit Neurooncology, German Cancer Consortium (DKTK), German Cancer Research Center (DKFZ), Heidelberg, Germany. [2]Clinical Cooperation Unit Neuropathology, German Cancer Consortium (DKTK), German Cancer Research Center (DKFZ), Heidelberg, Germany. [3]Department of Neuropathology, Heidelberg University Hospital, Heidelberg, Germany. [4]Faculty of Biosciences, Heidelberg University, Heidelberg, Germany. [5]Clinical Cooperation Unit Neuroimmunology and Brain Tumor Immunology, DKTK, DKFZ, Heidelberg, Germany. [6]Department of Neurology, Medical Faculty Mannheim, MCTN, Heidelberg University, Mannheim, Germany. [7]Department of Neurology, Heidelberg University Hospital, Heidelberg, Germany. [8]Department of Neuro-radiology, Heidelberg University Hospital, Heidelberg, Germany. [9]Junior Research Group Bioinformatics and Omics Data Analytics, German Cancer Research Center (DKFZ), Heidelberg, Germany. [10]Hopp Children's Cancer Center (KiTZ) and Division of Pediatric Neurooncology, German Cancer Consortium (DKTK), German Cancer Research Center (DKFZ), Heidelberg, Germany. [11]Department of Pediatric Oncology, Hematology, Immunology and Pulmonology, Heidelberg University Hospital, Heidelberg, Germany. [12]Department of Neurosurgery, Massachusetts General Hospital, Boston, Massachusetts. [13]Molecular Neuroimmunology Group, Department of Neurology, Heidelberg University Hospital, Heidelberg, Germany. [14]Neurology and Neurooncology Program, National Center for Tumor Diseases, Heidelberg University Hospital, Heidelberg, Germany.

F. Sahm and T. Kessler contributed equally to this article.

Corresponding Author: Tobias Kessler, Heidelberg University Hospital, Im Neuenheimer Feld 400, 69120 Heidelberg, Germany. E-mail: tobias.kessler@med.uni-heidelberg.de

Clin Cancer Res 2024;30:2974–85

doi: 10.1158/1078-0432.CCR-23-2907

Translational Relevance

Minimally invasive characterization of brain tumor genetic aberrations to guide diagnosis and targeted treatment is of major importance. Here we present an NGS panel sequencing approach to identify glioma tumor mutations and copy-number variations based on cfDNA from CSF and also provide a diagnostic classification format for liquid biopsies in brain tumors. The patient inclusion process was designed to represent clinical use cases in which patients with MRI-based suspicion of glioma presented at the study centers. Evaluation of this large and heterogeneous cohort enables identification of glioma subgroups and situations in which CSF cfDNA sequencing may be beneficial. In addition, ctDNA negative and nonmalignant cases allow estimation of patient numbers in which CSF cfDNA analysis remains inconclusive.

Molecular alterations together with MRI can guide CNS tumor diagnosis with high certainty. For example, the combination of chromosome (chr) 7 gain, chr 10 loss, *EGFR* amplification, and *TERT* promotor mutation without concomitant *IDH* mutation strongly argues for glioblastoma (3). However, accuracy of diagnosis and specific reporting strategies need to be improved for routine clinical application (10). Hence, routine detection of hallmark mutations from CSF could potentially accelerate diagnosis and treatment for brain tumors.

Various methods have been applied for analysis of CSF cfDNA including targeted sequencing (11), methylation profiling (12), next-generation sequencing (NGS; ref. 7) and nanopore sequencing (13). Whereas targeted and nanopore sequencing have advantages in speed of application, deep NGS combines the benefits of high accuracy and high throughput needed for valid tumor diagnosis upfront in newly diagnosed tumors. However, cfDNA sequencing is not applied in routine diagnostics yet and clear diagnosis algorithms are missing.

Here we present a CSF liquid biopsy approach in a prospective clinical study. Patients with MRI-based suspicion of glioma/recurrent glioma were included when molecular data were required to confirm diagnosis or specific genetic alterations. Inclusion of patients with impeded surgical tissue sampling was preferred, as depicted by a high fraction of patients with no solid tissue available or tissue derived from stereotactic biopsy (STX). We perform targeted NGS for combined detection of CNV profiles, single-nucleotide variants (SNV) at pre-defined gene loci in *IDH1/2*, *TERT*, *BRAF*, and H3K27 and small insertions/deletions (indel) identified via uninformed variant calling. These data are integrated to propose a diagnosis grading scheme (molecular-guided tumor classification) for cfDNA sequencing of adult glioma.

Materials and Methods

Patient cohort and study inclusion

Patients were prospectively recruited through the inpatient and outpatient care units at two German University Hospitals (Heidelberg, $n = 70$ and Mannheim, $n = 14$) between June 2020 and February 2023. The study was conducted in accordance with the Declaration of Helsinki and approved by the local Heidelberg (S-554/2018, S-130/2022) and Mannheim (2017-589N-MA) ethics committees. All patients signed informed consent for the usage of blood, CSF, and tumor tissue. Samples were collected in routine clinical care and results were reported to clinicians and patients. Clinical data were obtained from electronic patient records. The study was not preregistered.

Inclusion criteria were either MRI-based suspicion of a primary glioma ($n = 71$) or MRI-based suspicion of a recurrent/progressive glioma ($n = 14$) based on treating physicians evaluation. Exclusion criteria were age <18 years, and contraindications for lumbar puncture such as risk of herniation, anticoagulation, and thrombocyte count <50/nL as well as further risk factors based on the treating physician's discretion. The representativeness of those patients included in the study is presented in Supplementary Table S1. An overview of all cases is given in Supplementary Table S2.

Wet lab procedure and bioinformatics analysis

More details about the respective procedures can be found in Supplementary Materials and Methods.

CSF collection

Study materials were obtained by lumbar puncture ($n = 83$), puncture of Rickham reservoir ($n = 1$) or collected from extraventricular drain ($n = 1$). A standardized diagnostic workup of CSF chemistry (cell count, protein levels, glucose, lactate, quotient of albumin (qAlb) and presence of malignant cells) was performed for 84/85 samples.

DNA extraction

CSF cfDNA was isolated using the MagMAX Cell-free DNA Isolation kit (Thermo Fisher Scientific). Isolation was done either following the manual protocol provided by the manufacturer or automated isolation was performed on a KingFisher DuoPrime (Thermo Fisher Scientific).

Genomic DNA (gDNA) was isolated from blood leukocytes and formalin-fixed paraffin-embedded (FFPE) tissue using the Maxwell RSC Buffy Coat DNA Kit and Maxwell RSC DNA FFPE Kit on a Maxwell RSC 48 instrument (Promega) according to the manufacturer's recommendations.

Preparation of NGS libraries

For gDNA derived from FFPE tissue and blood leucocytes, NGS libraries were prepared using the SureSelect XT HS DNA Reagent Kit or SureSelect XT HS2 DNA Reagent Kit (Agilent). Hybrid capture–based targeted sequencing was performed using SureSelect Custom DNA Target Enrichment Probes (Agilent, capture region size ~1.3 Mb). The gene set covered by the panel was updated continuously during the study, resulting in different panel versions. Variant calling results were only reported for genes indicated in Supplementary Table S3, which were shared across all panel versions.

For CSF cfDNA, libraries were prepared using the SureSelect XT HS2 DNA Reagent Kit. The same SureSelect Custom DNA Target Enrichment Probes as for leukocyte and FFPE gDNA were used for hybrid capture–based target enrichment.

Sequencing

Sequencing was performed on a NovaSeq6000 instrument (Illumina). The NovaSeq 6000 SP, S1 or S2 Reagent Kit v1.5 (200 cycles) were used. The aimed raw on-target coverage was 15,000× for CSF cfDNA samples and 1,000 × −1,500× for matching blood controls or solid tissue FFPE samples. For raw on-target coverage calculation, the estimated percentage of reads on on-target was set to 65%.

Sequencing data analysis and variant calling

A customized pipeline was used for combined detection of CNVs, SNVs at genomic loci frequently altered in glioma (Supplementary Table S4) and SNVs/indels identified via uniformed variant calling in CSF cfDNA samples (Supplementary Fig. S1).

CNVs were visualized utilizing genome-wide on- and off-target reads from the not-deduplicated bam file (cnvkit, RRID:SCR_021917) and calls were made by manual revision.

SNVs at predefined gene loci were called in the not-deduplicated and deduplicated bam files (bcftools mpileup, RRID:SCR_002105) and calls were hard filtered for ADF/ADR ≥30 (not-deduplicated bam, allelic depths on the forward/reverse strand), ADF/ADR ≥8 (deduplicated bam), and variant allele frequency (VAF) ≥3% (both).

For uninformed variant calling, alterations in 38 genes frequently altered in glioma (Supplementary Table S3) were reported. The SomaticSeq (RRID:SCR_024891) variant classification model was trained for low input, low VAF CSF cfDNA samples (Supplementary Materials and Methods). From the SomaticSeq package, seven variant callers (Mutect2, VarScan2, Strelka2, VarDict, Scalpel, LoFreq, MuSE) were used for tumor-normal paired samples and six variant callers (Mutect2, VarScan2, Strelka2, VarDict, Scalpel, LoFreq) were used for tumor-only cases with no matching normal available. In both situations octopus variant caller (RRID:SCR_024890) was added to the model. To further increase specificity of uninformed variant calling, only variants were reported that in addition to passing SomaticSeq showed ≥10 hits of the locus in the COSMIC database (RRID:SCR_002260) or passed one of the following ClinVar (RRID:SCR_006169) filters: "Likely pathogenic", "Pathogenic", "Likely pathogenic, low penetrance", "Pathogenic, low penetrance", "Likely risk allele", "Established risk allele", "conflicting data from submitters".

For FFPE gDNA samples, copy-number variants were identified using the Infinium MethylationEPIC Kit (Illumina) and manual revision. SNVs at predefined loci and uninformed variant calling were performed using the same pipeline as described above for CSF cfDNA samples.

MRI

Processing of the anatomic MRI sequences (T1-w, cT1-w, T2-w, and FLAIR) was performed as described previously (14–16) and included automated deep learning–based brain extraction (16) followed by registration of the brain-extracted cT1-w, FLAIR, T2-w image volumes to the respective brain-extracted T1-w image volume using the linear image registration tool (FMRIB software library, RRID:SCR_002823) with spline interpolation and a 6-degree-of-freedom transformation. Subsequently, an automated deep learning–based voxel-wise segmentation was done using HD-GLIO tool (14, 15) to quantify the contrast-enhancing tumor volume and the nonenhancing T2-w/FLAIR signal abnormality volume.

Statistical analysis

All statistical analyses were performed in R (version 4.1.2, RRID:SCR_001905). Data visualization was done in R using the ggplot package (version 3.4.4, RRID:SCR_014601) and oncoprints from the ComplexHeatmap package (version 2.18.0, RRID:SCR_017270). $P < 0.01$ was used to indicate statistical significance.

Data and code availability

Sequence data have been deposited at the European Genome-phenome Archive (EGA), which is hosted by the European Bioinformatics Institute and the Centre for Genomic Regulation under accession number EGAS50000000060 (https://ega-archive.org; RRID:SCR_004944). Source code of the variant calling pipeline can be made available upon reasonable request.

Results

Workflow and patient cohort

We investigated the diagnostic potential of CSF cfDNA sequencing in patients presenting with suspicion of glioma at two neuro-oncological centers. Patients with MRI-based suspicion of a primary glioma ($n = 71$) or MRI-based suspicion of a recurrent/progressive glioma ($n = 14$) were included, while CSF collection was performed as part of the diagnostic procedure (Supplementary Fig. S2).

CSF cfDNA was available for all patients. In addition, we collected peripheral blood samples to perform paired sequencing whenever possible ($n = 75$, 88.2%). In 38 cases (44.7%), matching primary tumor was sequenced to compare alterations found in the CSF with the solid tumor (Supplementary Fig. S2).

Patients were allocated into cohorts according to the integrated diagnosis derived from clinical, radiological, and (if available) histopathologic findings of the corresponding solid tumor. Four cohorts were defined: glioblastoma ($n = 32$, 38%), other glioma ($n = 19$, 22%), nonmalignant ($n = 17$, 20%), and nondiagnostic ($n = 17$, 20%). For glioblastoma and other glioma cases, ultimate classification in the categories was tissue-based according to World Health Organization (WHO) 2021 (3) in 49/51 (96%) of the cases. Two patients (GB6 and GB13) were included in the study but died before surgery and the diagnosis of glioblastoma was based on imaging. Cases were included in the nonmalignant cohort after clear confirmation of a nonmalignant condition by the treating neurologist and sufficient likelihood of exclusion of a malignant condition. All cases with any doubt in a nonmalignant diagnosis were included in the "nondiagnostic" cohort.

Other glioma cases include H3 K27M-mutated DMG ($n = 5$); anaplastic pleomorphic xanthoastrocytoma ($n = 1$); astrocytoma, *IDH*-mutant, WHO grade 2/4 ($n = 2$), malignant astrocytoma not elsewhere classified ($n = 1$); oligodendroglioma WHO grade 2/3 ($n = 3$); pilocytic astrocytoma WHO grade 1 ($n = 2$); *IDH*-mutant glioma (not further classified, $n = 1$); malignant glial tumor (not further classified, $n = 1$); malignant glioma of the brainstem (not further classified, $n = 1$); anaplastic ependymoma ($n = 1$); posterior fossa ependymoma type B (PFA; $n = 1$). Nonmalignant conditions were inflammatory lesions ($n = 6$); gliosis ($n = 2$); myelitis ($n = 2$); ischemia ($n = 1$); neurodegeneration ($n = 1$); FLAIR hyperintensities ($n = 2$); peripheral paresis of cranial nerve VII ($n = 1$); neurosarcoidosis ($n = 1$), myelopathy ($n = 1$). Patients for whom no confirmed diagnosis was reached after diagnostic workup were stratified into a nondiagnostic cohort and analyzed separately.

After CSF sampling and cfDNA isolation, targeted sequencing was conducted using an approximately 1.3 Mb gene panel. This was followed by the joined analysis of genome-wide copy-number profiles, genomic loci frequently altered in glioma (referred to as "special positions"), and uninformed short variant calling (**Fig. 1A**). The short variant calling pipeline utilized for uninformed calling has been previously optimized for low VAFs and small input amounts of cfDNA (Supplementary Fig. S1; Supplementary Materials and Methods).

Molecular-guided tumor classification

A strategy for clinical interpretation of molecular data derived from CSF cfDNA sequencing was developed. CNVs, SNVs at predefined loci and panel-wide uninformed variant calling results were combined to

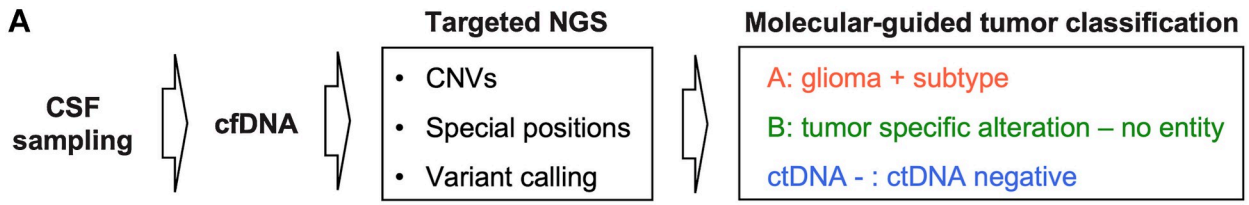

B

	A			B	ctDNA -
Glioblastoma	chr7 gain	+	TERT promotor chr10 loss EGFR amplification IDH wt	Characteristic + Other CNV TERT promotor	- Characteristic CNV - Characteristic Mutation ≤1 Other CNV
Other glioma	Histone H3 K27M IDH1 R132 chr7 gain	 + +	 chr1p/19q codeletion BRAF V600E	IDH1 R132 TERT promotor ≥2 Other CNV	- Characteristic CNV - Characteristic Mutation ≤1 Other CNV

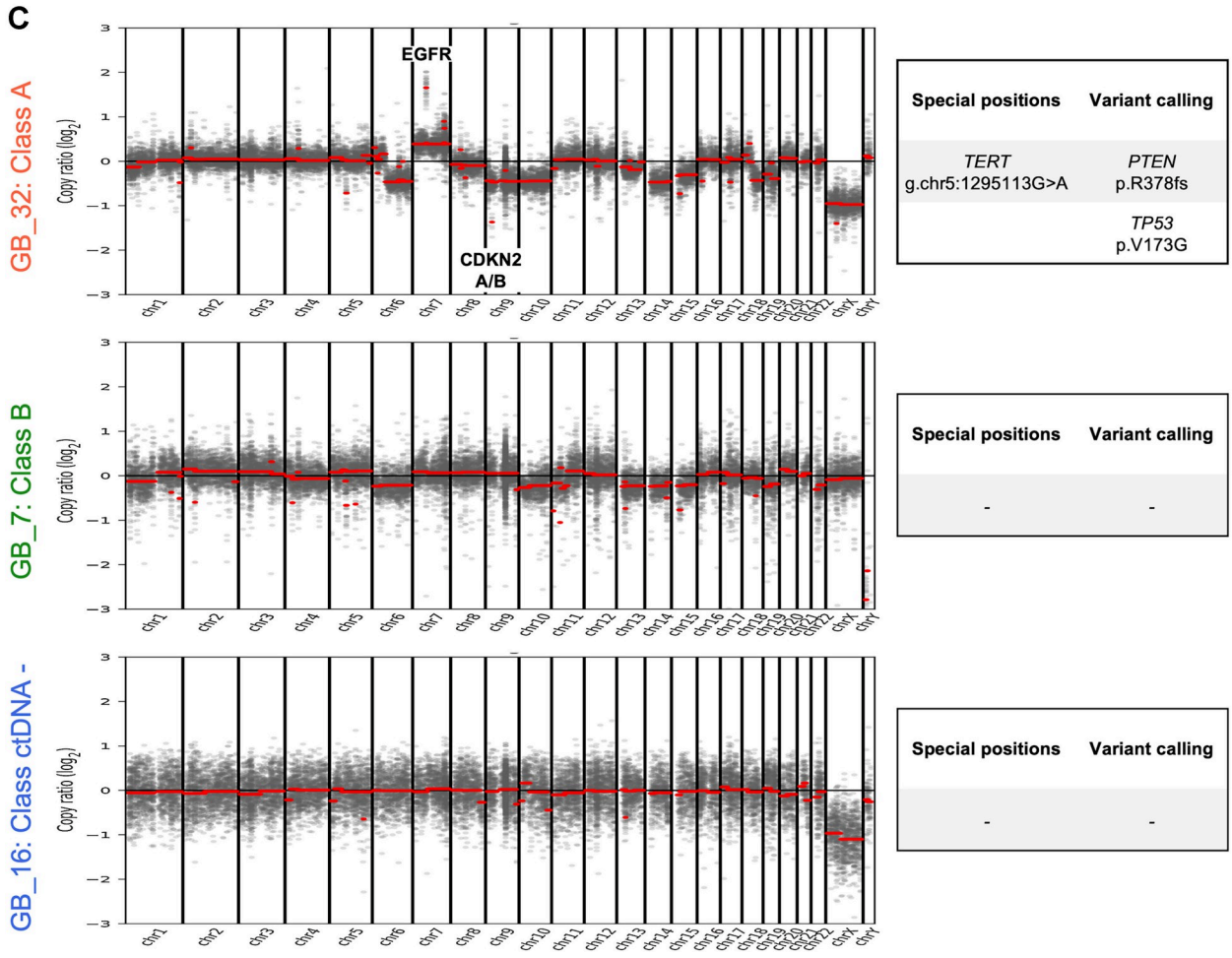

Figure 1.

cfDNA sequencing procedure and molecular-guided tumor classification. **A,** Key steps of the wet lab procedure and sequencing data analysis. CNVs, SNVs at predefined gene loci (special positions), and uninformed variant calling were combined to obtain a molecular-guided tumor classification. **B,** Combinations of genetic alterations sufficient for the respective classification categories. **C,** CNVs, special positions, and variants identified via uninformed calling for representative examples of class A (top), class B (middle), and ctDNA negative (bottom) cases.

obtain a molecular-guided tumor classification. For this, we analyzed the per sample occurrence of 67 characteristic genetic aberrations that were described in the 2021 WHO Classification of Tumors of the Central Nervous System (Supplementary Table S3). All samples were classified into three groups: (A) glioma-subtype classification possible; (B) tumor-specific alteration found, no entity assignment possible and (ctDNA) ctDNA negative, no tumor defining alterations found (**Fig. 1A**).

Different combinations of alterations were sufficient for a classification as type A, B, or ctDNA (**Fig. 1B**). Class A, B, and ctDNA—glioblastomas showed characteristic combinations of genetic features (**Fig. 1C**). In case GB_32, chr7 gain with *EGFR* amplification, chr9p loss with *CDKN2A/B* deletion, chr10 loss, *TERT* promotor mutation, *PTEN* and *TP53* mutation was identified, which was in combination specific for a glioblastoma (A classification). Sample GB_7 showed unspecific CNVs, resulting in B classification. No tumor specific alterations were seen in sample GB_16, leading to classification as ctDNA negative.

Molecular-guided tumor classification of glioblastoma and other glioma cohorts

Type A molecular-guided tumor classification was achieved for 62.5% ($n = 20$) of the cases in the glioblastoma cohort and 26.3% ($n = 5$) of cases in the other glioma cohort (**Fig. 2A**). Type B

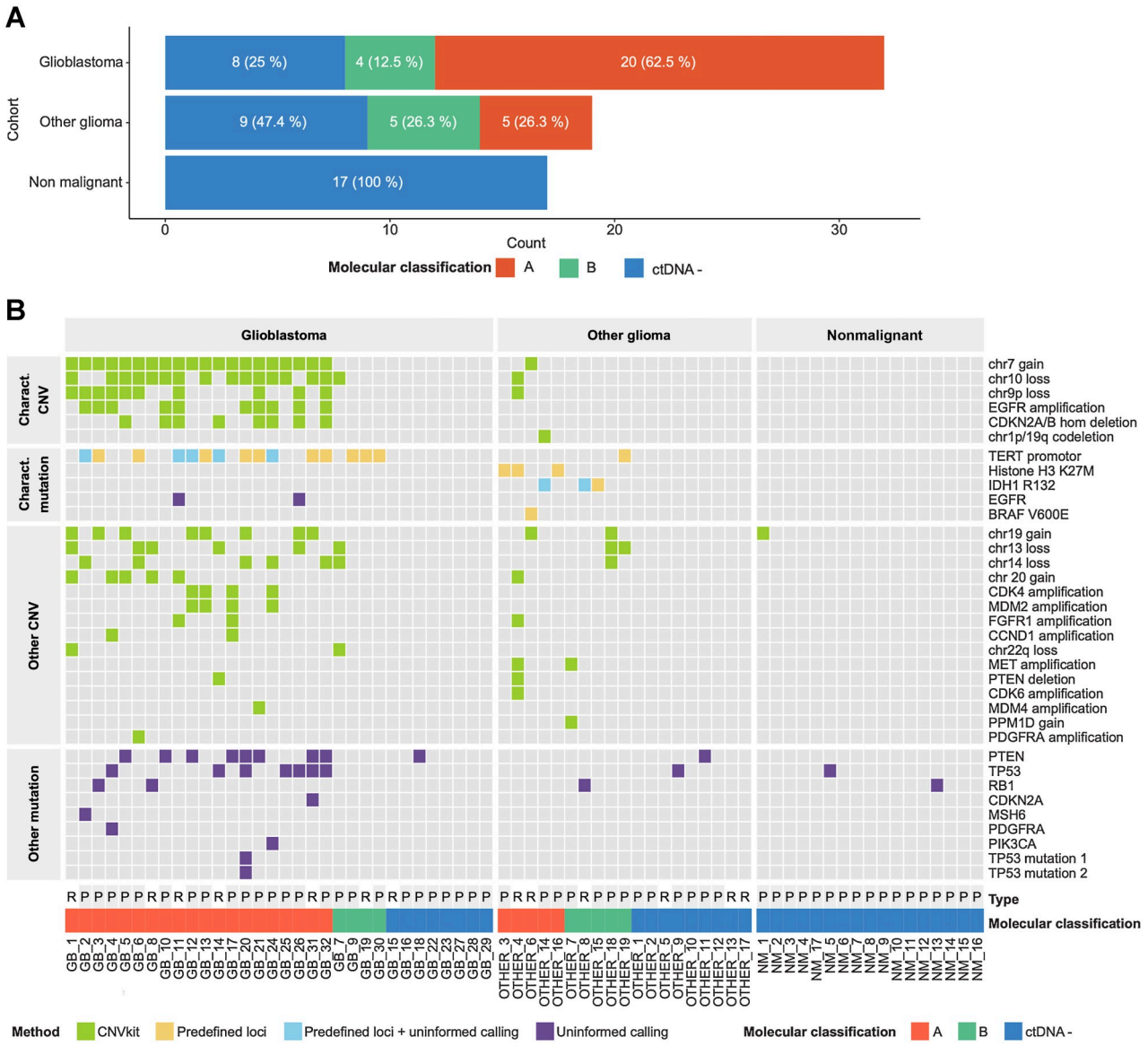

Figure 2.

Classification of glioblastoma, other glioma, and nonmalignant cohorts. **A,** Proportion of class A, B, or ctDNA negative cases in the glioblastoma, other glioma, and nonmalignant cohorts. **B,** Oncoprint of all identified genetic alterations. Variants were either identified via manual review of CNV profiles, SNVs at predefined loci (special positions), or uninformed variant calling. In some cases, SNVs at predefined loci were also identified via uninformed variant calling. Samples are grouped by molecular-guided classification within each cohort. P, primary tumor; R, recurrent tumor.

classification was available in an additional 12.5% ($n = 4$) of glioblastoma and 26.3% ($n = 5$) of other glioma cases (**Fig. 2A**).

Two subgroups of H3 K27M-mutant DMG and *IDH*-mutant gliomas were identified in the other glioma cohort. For H3 K27M-mutant DMG ($n = 5$), 3/5 cases achieved a type A classification and 2/5 were classified as ctDNA negative (60% of the cases with type A classification). For *IDH*-mutant gliomas ($n = 6$), 1/6 type A and 2/6 type B classifications were observed (50.0% with type A/B classification).

For each case, genetic aberrations identified via our integrated sequencing approach are depicted in **Fig. 2B**. Class A cases showed high amounts of characteristic CNVs (mean: 3.1/glioblastoma, 0.8/other glioma) and characteristic mutations (mean: 0.6/glioblastoma, 0.8/other glioma). Class B samples still contained a considerable number of specific mutations (mean: 0.75/glioblastoma, 0.6/other glioma). Characteristic alterations identified in both cohorts include copy-number variants (e. g. chr7 gain, chr10 loss, chr9p loss, *EGFR* amplification, *CDKN2A/B* homologous deletion and chr1p/chr19q codeletion) or mutations (e. g. *TERT* promotor, Histone H3 K27M, *IDH1* R132, *EGFR*; **Fig. 2B**). Other copy-number variants (e. g. chr19 gain, chr13 loss, chr14 loss, chr20 gain, *CDK4* amplification, *MDM2* amplification) or mutations (e.g., *TP53*, *PTEN*) frequently altered in primary brain gliomas were also identified in class A/B cases of both cohorts. No characteristic CNVs/mutations were identified in nonmalignant samples (**Fig. 2B**). Other mutations were identified rarely in the nonmalignant cohort and most probable indicate false-positive calls.

The positive and negative predictive values, as well as false-positive and false-negative rates of a type A/B classifications were calculated for glioblastoma, other glioma and nonmalignant cases. Calculations were also performed for other glioma subgroups H3 K27M-mutant DMG and *IDH*-mutant tumors. High reliability of a class A/B classification was represented by 100% positive predictive value and 0% false-positive rate for all glioma groups. On the other site, false-negative rates ranging between 25.0% and 50.0% for gliomas and a considerable low positive predictive value (50.0%) and false-positive rate (33.3%) for nonmalignant cases indicate that a ctDNA—classification cannot rule out glioma diagnosis (**Table 1**).

Comparison with matching tissue

For 81.3% ($n = 26$) of glioblastoma and 63.2% ($n = 12$) of other glioma cases, matching solid tumor tissue was available and sequenced for comparison of molecular features (Supplementary Fig. S3). In 25 primary cases, tissue was collected during surgery after lumbar puncture (median: + 7 days, range: 0 days; + 42 days). In three cases of primary glioma (GB_3, GB_16, OTHER_1), tissue was obtained via STX 29 days, 34 days, and 9 days before CSF collection. In 10 recurrent/progressive cases, tissue was collected at primary diagnosis (median: −337.50 days, range: −1,702 days; −57 days). For all matching solid tissue samples, CNVs were derived from Illumina EPIC array, because targeted sequencing coverage was too low for robust CNV estimations based on on-and off-target reads. SNVs at predefined gene loci and SNVs/indels from uninformed variant calling were available from targeted sequencing.

Comparison of molecular features between CSF and matching solid tissue was performed separately for CNVs, SNVs at predefined gene loci and pipeline called SNVs/indels. In the glioblastoma cohort, the overlap between CSF and matching solid tissue was highest for CNVs (48%, $n = 134$ CNVs in total identified), followed by SNVs at predefined gene loci (44%, $n = 18$ SNVs in total identified) and variants from uninformed variant calling (14%, $n = 43$ SNVs/indels in total identified; **Fig. 3A**). For the other glioma cohort, the overlap was 44% for SNVs at predefined gene loci ($n = 9$ SNVs in total identified), 26% for CNVs ($n = 27$ CNVs in total identified) and 8% for variants from uninformed variant calling ($n = 12$ SNVs/indels in total identified; **Fig. 3A**).

In both cohorts, overlap was highest in cases with type A molecular-guided tumor classifications (**Fig. 3B** and **C**). Class B samples showed only few shared alterations and no overlapping variants were found in samples which were CSF ctDNA negative (**Fig. 3B** and **C**).

Diagnostic CNVs are enriched for clonal variants, while other CNVs include potentially subclonal variants. Comparison of diagnostic CNVs versus other CNVs was performed for glioblastoma cases with classification A and matching solid tissue available. Solid-CSF overlap was significantly higher for diagnostic CNVs (44/54, 81.5%) versus other CNVs (16/37, 43.2%; $P < 0.01$, Fisher exact test). These findings suggest tumor heterogeneity could be partially responsible for differences between solid tissue and CSF cfDNA.

When comparing primary and recurrent glioblastomas, we did not observe significant differences regarding frequency of type A/B classifications (recurrent cases: 85.7% A/B classifications, primary cases: 72.0% A/B cases, $P = 0.6464$, Fisher exact test). In concordance, CSF-solid overlap of combined variants (CNVs, special positions and variants derived from uninformed variant calling) was also not significantly different for recurrent cases (21/43 shared variants, 48.8%) versus primary glioblastomas (57/152 shared variants, 37.5%; $P = 0.6833$, Fisher exact test), indicating longitudinal stability of the described genetic alterations.

CSF private diagnosis-guiding alterations were observed in 6 patients (**Fig. 3B** and **C**). Such alterations include *TERT* promotor mutations ($n = 3$) and *EGFR* amplifications ($n = 2$). In one additional patient (OTHER_15), an *IDH1* R132S mutation was only detected in CSF and not identified in the corresponding solid tumor. Retrospective analysis of the solid tumor revealed low tumor cell content in the tissue used for sequencing. Therefore, we assume that the absence of *IDH1* mutation is rather due to limited tumor DNA content in the solid tissue, than due to a false-positive call in CSF cfDNA sequencing.

In two cases (GB_15, GB_16), we observed zero or only one characteristic genetic alteration in the solid tissue (**Fig. 3B**). Therefore, at least some ctDNA-negative classified glioblastoma cases could be explained by a noncharacteristic genetic profile of the solid tumor. In these samples, tumor classification based on molecular markers remains difficult and classical histopathology is required.

Table 1. Predictive values and false-positive/negative rates of molecular-guided tumor classification.

Diagnosis	ctDNA class	*N*	PPV	NPV	FPR	FNR
Glioblastoma	Class A/B	20	1	0.818	0	0.250
	ctDNA negative	12				
Other glioma	Class A/B	5	1	0.845	0	0.474
	ctDNA negative	14				
H3 K27M DMG	Class A/B	3	1	0.969	0	0.400
	ctDNA negative	2				
IDH-mut glioma	Class A/B	2	1	0.954	0	0.500
	ctDNA negative	4				
Nonmalignant	ctDNA negative	17	0.500	1	0.333	0
	Class A/B	0				

Note: Indicated statistical parameters were calculated for the labeled diagnoses and molecular classification types.
Abbreviations: FNR, false-negative rate; FPR, false-positive rate; NPV, negative predictive value; PPV, positive predictive value.

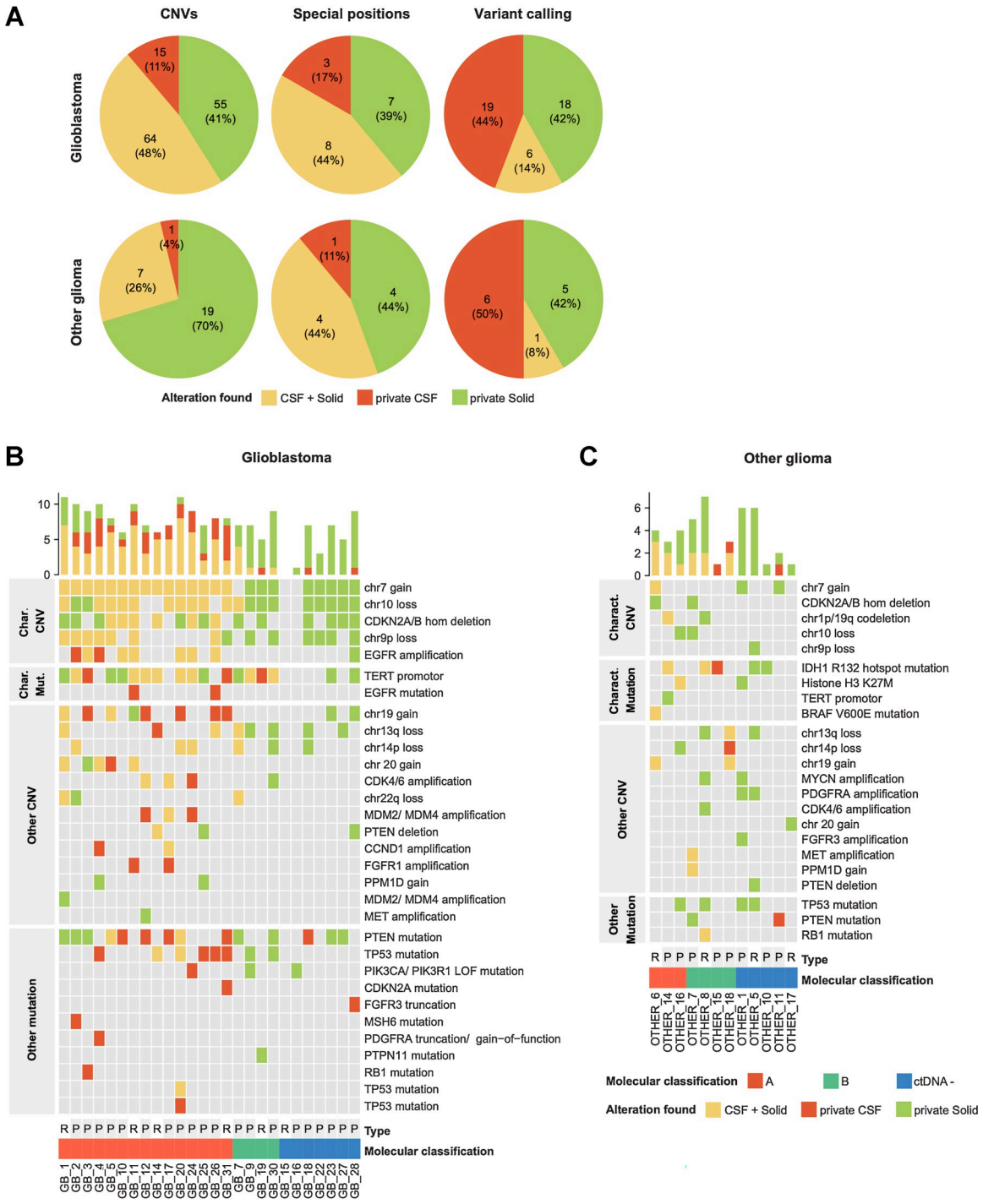

Figure 3.

Comparison between CSF and matching solid tumor. **A,** For cases where matching solid tissue was available, the overlap between CSF and solid tissue calls was analyzed separately for CNVs, SNVs at predefined gene loci (special positions), and SNVs/indels identified via uninformed variant calling. **B** and **C,** Oncoprints of identified variants that were either shared between CSF and matching solid or private to one or the other. P, primary tumor; R, recurrent tumor. **B,** Glioblastoma cohort. **C,** Other glioma cohort.

pt?>Clinical reports of recurrent cases in the joint glioblastoma and other glioma cases were checked for reported progression/pseudoprogression at the timepoint of CSF draw and such information were available for 12/14 cases (Supplementary Table S2). We identified three cases of pseudoprogression (GB_19), stable disease (GB_15), and remission (OTHER_17) versus nine cases with reported progression at CSF draw. Interestingly, 2/3 ctDNA negative and 1/3 type B classifications

were made for nonprogressive recurrent cases, while progressive cases achieved type A/B classification in 7/9 cases.

Patients who are ineligible for surgery are well represented in the study cohort, indicated by the high rate of stereotactic biopsies performed ($n = 16$, 42.1% of cases with matching solid tumor available). Even though, intraoperative risks are much lower for STX, it is still not risk-free and diagnostic sensitivity is lower than collecting tumor tissue via surgery (17). We observed competitive reliability of CSF cfDNA sequencing for patients undergoing STX, with 12/16 cases achieving class A/B classification in the CSF (75.0%).

CSF chemistry, MRI sequencing, and clinical parameters

We collected basic CSF chemistry parameters such as cell count ($n = 84$), protein ($n = 84$), glucose ($n = 81$), and lactate ($n = 80$) levels, CSF/serum qAlb ($n = 78$), the amount of cfDNA ($n = 83$) and CSF ($n = 81$) as well as presence of malignant cells ($n = 85$). From all collected parameters, only CSF lactate levels and cfDNA amount differed significantly when comparing glioblastoma versus nonmalignant cases (**Table 2**). Glioblastoma cases showed significantly higher CSF lactate ($P < 0.01$, Wilcoxon rank-sum exact test) and cfDNA ($P < 0.01$, Wilcoxon rank-sum exact test) levels (**Table 2**). Also, microscopic evidence of malignant cells was exclusively found in four glioblastoma cases. No significant differences were found when comparing the other glioma cohort to nonmalignant cases at the indicated alpha level (**Table 2**). One might assume that CSF amount correlates with total cfDNA yield; however, we did not see this correlation in our overall cohort (Supplementary Fig. S4), which is most probably due to the limited sample size and diverse tumor entities.

CSF chemistry features between A/B classified and ctDNA negative cases were compared. In the glioblastoma cohort, cfDNA amount was significantly higher in class A/B samples ($P < 0.01$, Wilcoxon rank-sum exact test), while no such trend was observed for the other glioma cohort.

In 30 glioblastoma cases (94%) and 13 other glioma cases (68%), MRI datasets were available for the period <2 weeks prior CSF collection. Contrast-enhancing volume, edema volume, tumor tissue volume, and combined volume was calculated as described previously (14). Interestingly, no difference of these parameters was observed between type A/B classified and ctDNA negative samples in both cohorts (**Table 2**).

For 41 glioblastoma and other glioma cases, distance between the tumor and CSF space was determined (Supplementary Table S2). We compared molecular-guided tumor classification of tumors touching the CSF space (= 0 mm distance) versus cases with normal appearing brain parenchyma separating tumor from CSF space (>0 mm distance). Frequency of type A/B classification was 23/27 (85.2%) for cases touching the CSF space versus 5/14 (35.7%) for nontouching cases (P value < 0.01, Fisher exact test; Supplementary Fig. S5). Importantly, the representation of glioblastoma cases in the compared groups was not significantly different (0 mm distance: 21/27 glioblastomas, >0 mm distance: 9/14 glioblastomas, $P = 0.4629$, Fisher exact test).

Bioinformatically, no significant differences in on-target read coverage was observed between glioma cohorts and nonmalignant controls as well as between type A/B and ctDNA negative cases (**Table 2**).

We did not observe statistical difference in type A/B classifications for patients with glioblastoma with steroid administration for 2 weeks prior CSF draw (12/15 class A/B cases, 80.0%) versus patients with steroid-naïve glioblastoma (10/15 class A/B cases, 66.7%, P value = 0.6817, Fisher exact test; Supplementary Table S2).

Nondiagnostic cohort

CSF cfDNA sequencing was also performed for 17 patients with a suspicion of glioma on MRI scan, but no tissue material available for confirmation of diagnosis. We asked, whether CSF cfDNA sequencing can give insights into tumor entity and molecular features of such cases. Indeed, in 23.5% ($n = 4$) of these cases a type A/B classification was made (**Fig. 4A**).

In one type A classified case, a histone H3 K27M mutation was detected, which is suggestive of DMG (**Fig. 4B**). Three other cases achieved type B molecular-guided classification. In these cases, *IDH1* R132 ($n = 2$) or *IDH2* R172 ($n = 1$) mutations were identified, which are highly suggestive for *IDH*-mutant glioma (**Fig 4B**). For the H3 K27M-mutated DMG (**Fig. 4C**) and one *IDH*-mutant glioma (**Fig. 4D**) integration of CSF cfDNA sequencing results with MRI findings led to the establishment of an integrated clinical diagnosis by the molecular tumor board, which was guiding further treatment and follow-up.

Comparison with existing methods for CSF cfDNA-based glioma diagnostics

We performed literature research to compare our workflow with available state-of-the-art methods (Supplementary Materials and Methods; Supplementary Fig. S6; Supplementary Table S5). When we consider type A/B classified cases ctDNA positive, our approach achieves a sensitivity of 66.7% across combined glioblastoma and other glioma cohorts. This is the highest detection rate of a NGS approach compared with the selected literature (Supplementary Fig. S6; Supplementary Table S5). Sensitivity is currently only outperformed by digital droplet PCR (ddPCR), which is highly sensitive but restricted to analysis of predefined genetic aberrations.

Importantly, we did not encounter any sample dropouts, which is regularly observed in previous studies (Supplementary Table S5). Our pipeline requires lower CSF cfDNA amounts, which enables analysis in cases with minimal cfDNA available: the lowest total CSF cfDNA input amount necessary for archiving a type A classification was 0.41 ng for glioblastoma, 0.25 ng for *IDH*-mutant glioma, and 0.22 ng for H3 K27M DMG.

Discussion

Here, we present CSF cfDNA sequencing in a clinical setting where patient inclusion was designed to mimic clinical use cases of patients presenting at large neurooncological centers with suspicion of glioma but unclear initial diagnosis and/or ineligibility to surgery. Therefore, many cases were later identified as nonmalignant conditions ($n = 17$) or remained nondiagnostic ($n = 17$). Recurrent cases represent a relevant proportion of our cohort, and these patients were mostly included when verification of primary tumor mutations was desired at recurrence.

The here presented pipeline efficiently integrates whole-genome CNV profiles, variants at predefined gene loci and uninformed short variant calls, thereby maximizing the amount of genetic information derived from CSF cfDNA. One of the key benefits of this approach is that all three methods require targeted sequencing data only, eliminating sample splitting for different methods. We want to emphasize that the gene panel and library preparation workflow of our pipeline are similar to the ones currently used in molecular neuropathology of solid gliomas. Consequently, immediate and combined analysis of CSF cfDNA samples with solid tissue results in rapid turnover times of approximately 5 days between CSF collection and molecular-guided tumor classification (Supplementary Fig. S7).

Table 2. Case characteristics.

	Glioblastoma				Other glioma				Suspicion of glioma		Nonmalignant
Patient characteristics											
Cases	32				19				17		17
Sex (% female)	41				74				35		71
Age (median) (range)	63 (39–86)				36 (21–74)				58 (26–73)		51 (23–80)
Primary (%)	78				68				94		100
	Total	**p_val1**	**Class A/B**	**ctDNA–**	**p_val2**	**Total**	**p_val1**	**Class A/B**	**ctDNA–**	**p_val2**	**Total**	**Total**
CSF chemistry												
Cell count (range)	2 (1–421)	0.627	2 (1–421)	2 (1–20)	0.821	2 (1–80)	0.584	2 (1–5)	2 (1–80)	0.798	1 (1–6)	2 (1–47)
Protein (mg/dL) (range)	70.9 (12.7–2,636.6)	0.019	80.1 (12.7–2,636.6)	58.7 (19.3–340)	0.586	39.9 (27.5–500)	0.461	43.8 (29.8–500)	36.4 (27.5–205)	0.497	51.5 (28.4–86.6)	39.2 (23.6–115.8)
Glucose (mg/dL) (range)	68 (9–200)	0.065	70 (9–200)	64 (43–78)	0.239	59 (17–73)	0.554	62 (17–73)	54 (49–65)	0.367	59 (53–100)	62 (47–68)
Lactate (mmol/L) (range)	1.7 (1.27–12.5)	**0.010**	1.8 (1.29–12.5)	1.6 (1.27–1.91)	0.144	1.5 (1.11–6.66)	0.270	1.5 (1.11–6.66)	1.5 (1.15–2.08)	0.824	1.4 (0.95–1.8)	1.4 (1.04–2.87)
qAlb (range)	10.2 (1.9–429.8)	0.066	12.1 (1.9–429.8)	8.0 (2.3–61.3)	0.511	6.1 (3.2–161)	0.258	6.1 (4.4–161)	6.0 (3.2–30.3)	0.370	6.6 (3.6–12.3)	5.3 (3.17–19.14)
cfDNA (ng/mL) (range)	0.43 (0.02–70.00)	**0.001**	0.47 (0.02–70.00)	0.10 (0.03–0.48)	**0.009**	0.15 (0.03–1.89)	0.038	0.12 (0.03–1.89)	0.37 (0.05–1.10)	0.549	0.11 (0.03–0.42)	0.08 (0.01–0.60)
CSF (mL) (range)	5 (2–8)	0.542	5 (2–8)	6 (3.5–7)	0.290	5 (1.5–35)	0.421	5 (1.5–8)	5 (2–35)	0.506	6.2 (4–9)	6 (1,8–9)
Malignant cells (% of cases)	$n = 4$ (12.5)	–	$n = 3$ (12.5)	$n = 1$ (12.5)	–	$n = 0$ (0)	–	–	–	–	$n = 0$ (0)	$n = 0$ (0)
MRI												
CE vol × 10^3 (mm^3) (range)	10.1 (0–63.8)	–	5.2 (0.1–54.9)	17.6 (0–63.8)	0.680	0.5 (0–24.1)	–	0.6 (0–24.1)	0.3 (0–6.8)	0.744		
Edema vol × 10^3 (mm^3) (range)	37.6 (3.8–159.6)	–	33.7 (3.8–159.6)	53.9 (5.4–142.7)	0.377	15.4 (0–159.8)	–	25.5 (0–73.6)	15.4 (7.9–159.8)	0.937		
Tissue vol × 10^3 (mm^3) (range)	67.4 (6.4–192.0)	–	57.0 (6.4–159.8)	80.1 (8.2–192.0)	0.308	17.5 (0–166.6)	–	28.6 (0–97.7)	17.1 (7.9–166.6)	1.000		
Whole vol × 10^3 (mm^3) (range)	67.4 (6.4–192.0)	–	57.0 (6.4–159.7)	80.1 (8.2–192.0)	0.308	17.5 (0–166.6)	–	28.6 (0–97.7)	17.1 (7.9–166.6)	1.000		
Brain vol × 10^3 (mm^3) (range)	1,476 (1,276–1,724)	–	1,487 (1,276–1,657)	1,466 (1,344–1,724)	0.832	1,438 (1,208–1,722)		1,471 (1,296–1,626)	1,396 (1,208–1,722)	0.589		
Sequencing												
Coverage (range)	281 (101–1,527)	0.700	319 (101–1,527)	230 (171–524)	0.357	297 (30–449)	0.573	300 (151–449)	225 (30–352)	0.243	205 (82–334)	279 (147–835)

Note: Patient characteristics, CSF chemistry parameters, tumor volumes derived from MRI and on-target coverage after deduplication. p_val1: comparison of glioblastoma/other glioma cohorts to nonmalignant cohort (Wilcoxon rank-sum test, alpha level ≤ 0.01). p_val2: comparison of A/B versus ctDNA negative cases within the glioblastoma/other glioma cohorts (Wilcoxon rank-sum test, alpha level ≤ 0.01). CE vol: contrast enhancing volume. Numbers in bold are statistically significant.

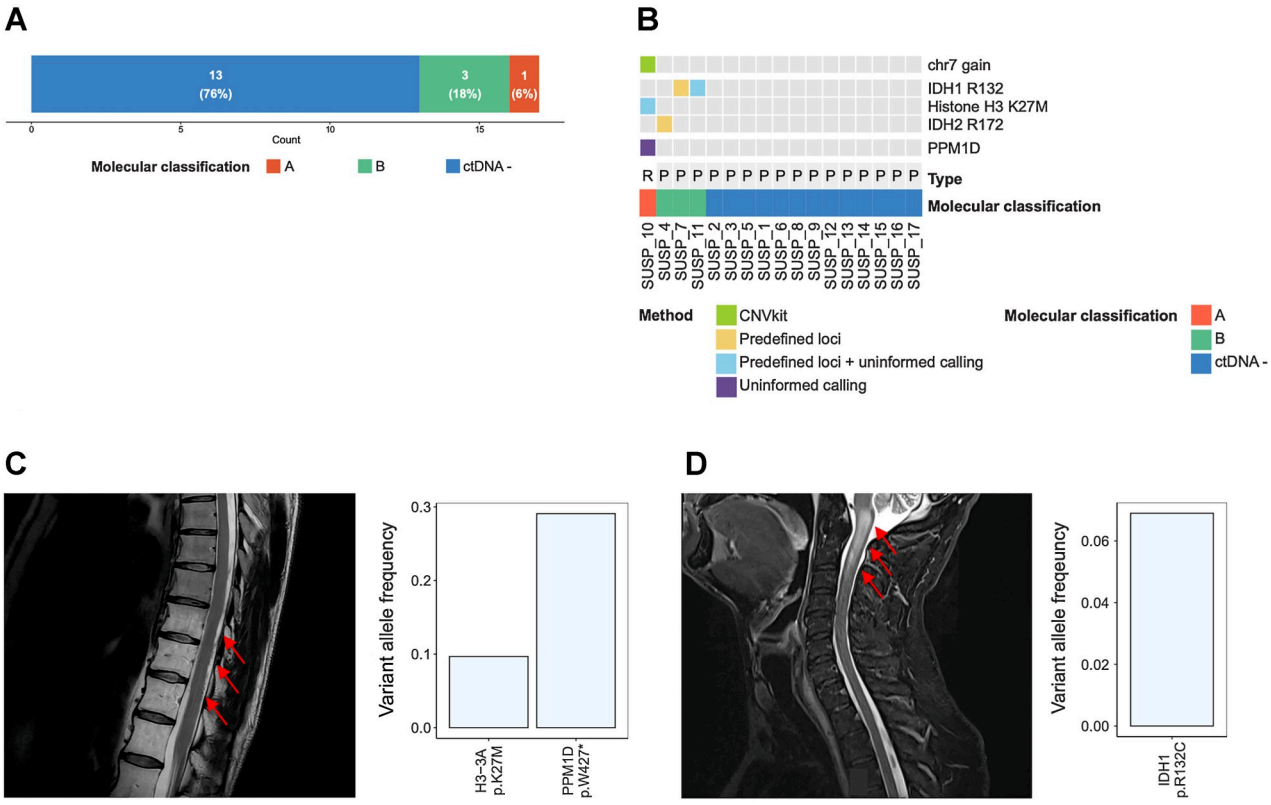

Figure 4.

Nondiagnostic cases. **A,** Molecular-guided tumor classification for all samples in the nondiagnostic cohort. **B,** Oncoprint of identified CNVs, SNVs at predefined loci (special positions), and SNVs/indels identified via uninformed variant calling. P, Primary tumor; R, recurrent tumor. **C** and **D,** Representative MRI and VAF for two cases where integrated clinical diagnosis was made based on CSF cfDNA sequencing results and MRI findings. **C,** Case SUSP_10: H3 K28M-mutated DMG. **D,** Case SUSP_11: *IDH*-mutant glioma.

Modifications of the NGS panel for future applications are straightforward. Capture probes for hybrid capture can simply be added or exchanged, without changing the wet lab or bioinformatics procedure.

The here introduced molecular-guided tumor classification enabled partially overcoming previously reported sensitivity limitations of CSF cfDNA sequencing, which was based on variant calling at single or predefined gene loci (Supplementary Fig. S6; Supplementary Table S5). Altogether, 75.0% ($n = 24$) of glioblastoma and 52.6% ($n = 10$) of other glioma cases were either A or B classified only based on CSF cfDNA sequencing.

The success of molecular classification varied depending on the tumor type. Glioblastomas were more frequently classified as type A or B compared with other tumors.

Within the other glioma cohort, we identified subgroups of tumors with specific characteristic mutations, such as *H3* K27M or *IDH1* R132 mutations, which showed the highest degree of type A/B classification. Most probably, this is due to variants at specific gene loci being identified with higher sensitivity than uninformed variant calling. Entity-dependent differences could also result from differential ctDNA emission of certain tumors. For example, infiltrative growth and high proliferation (resulting increased cell death via apoptosis/necrosis) could influence the amount of ctDNA emitted into CSF.

We opted for a more conservative and precise reporting procedure to keep false-positive calls in nonmalignant samples low. Therefore, variants in nonmalignant samples were only identified via uninformed variant calling. Importantly, the negative predictive value was 100% for nonmalignant samples and no samples were misclassified as tumors, underscoring the specificity of our integrated molecular classification approach.

A considerable number of cases in our cohort represent recurrent tumors. In most cases, no recurrent solid tumor material is available, and it is unclear whether molecular alterations described at initial diagnosis are still present. However, knowledge of certain mutations at recurrence is from special interest when considering individualized treatment options. For example, CSF cfDNA sequencing could be applied to monitor treatment response for alteration-specific immunotherapies (18, 19) or targeted treatments (20). Indeed, treatment-guiding alterations were identified via CSF cfDNA sequencing of recurrent tumors and frequency of type A/B classifications was not significantly different for primary versus recurrent cases. Interestingly, no significant difference in CSF-solid overlap was identified between primary and recurrent tumors, indicating that most of the investigated alterations remain stable over time.

The overlap of individual variants between CSF and matching solid tissue was limited, with CNVs and variants at predefined gene loci showing higher overlap compared with uninformed variant calling. In addition, CSF private variants (which are always suspect for false-positive calls) occurred less frequently with these two methods. This highlights the importance of considering the calling method when assessing reliability of identified variants. For

example, CNVs and variants called at predefined loci can be interpreted with higher reliability than SNVs/indels identified in uninformed variant calling.

Our findings of limited overlap of genetic variants in CSF and corresponding solid tumor tissue were in concordance with others (Supplementary Fig. S6; Supplementary Table S5). Reduced overlap can be attributed to methodologic limitations, such as lower sensitivity of variant calling and a higher rate of false positives in CSF cfDNA samples. We hypothesize, that moderate CSF-solid overlap could at least partially be caused by tumor heterogeneity. In accordance, we observe higher overlap for characteristic CNVs (enriched for clonal aberrations) versus other CNVs.

Clinical reports revealed pseudoprogression, stable disease, and remission in three recurrent glioma cases, which were associated with a ctDNA negative classification. This indicates the ability of cfDNA sequencing to distinguish progressive from nonprogressive gliomas, as demonstrated by others (8).

A considerable number of patients had solid tumor tissue available from STX, and we observed comparable tumor classification reliability with CSF cfDNA sequencing. Further studies will investigate whether our technical workflow can supplement or even replace STX in certain situations.

One goal of our study was the identification presequencing markers indicating CSF ctDNA positivity. Total cfDNA amount was significantly higher for class A/B cases at least in patients with glioblastoma. Moreover, detailed analysis of MRI data showed significantly higher amounts of type A/B classified cases for tumors with direct contact to the CSF space, which has also been described by others (7). For glioblastoma cases, we analyzed association of tumor localization in the brain with molecular-guided classification (Supplementary Fig. S8). No class A/B high regions were identified. Taken together, these findings indicate that proximity to the CSF space, and not tumor localization, size or blood–brain barrier disruption, is indicative of ctDNA shed into CSF.

We further investigated cases where no tumor tissue was available for molecular diagnostics (nondiagnostic cohort). The reasons for not performing a tissue sampling were low probability of glioma, tumor location, risk of neurologic deterioration through surgery and/or reduced performance status of the patient. In such situations, a CSF liquid biopsy can be considered to enable the identification of tumor-specific genetic alterations. Most nondiagnostic cases were classified as ctDNA negative. However, distinguishing correct from false negatives is not possible with our approach. Therefore, combination of our pipeline with more sensitive methods (such as ddPCR) is needed for routine clinical applications.

In conclusion, we established a molecular classification approach for CSF cfDNA sequencing that could aid diagnosis in cases where acquisition of tissue is difficult. Further studies need to be performed to address the question of noninferiority compared with tissue biopsy for difficult to reach anatomic locations.

Authors' Disclosures

G.M. Shankar reports grants from NIH during the conduct of the study as well as personal fees from Depuy Synthes/J&J and grants from NuVasive and Cervical Spine Research Society outside the submitted work; in addition, G.M. Shankar has a patent for US20170369939A1 issued. B. Wildemann reports grants from Deutsche Forschungsgemeinschaft, German Ministry of Education and Research, Baden-Württemberg Ministry for Science, Research and Art, Dietmar Hopp Foundation, Klaus Tschira Foundation; grants and personal fees from Merck and Novartis; and personal fees from Alexion, INSTAND, and Roche outside the submitted work. W. Wick reports personal fees from Servier and Roche outside the submitted work. F. Sahm reports grants from Assmus Foundation during the conduct of the study. T. Kessler reports grants from Else Kröner-Fresenius Foundation and German Research Foundation during the conduct of the study as well as grants from Hertie Foundation outside the submitted work. No disclosures were reported by the other authors.

Authors' Contributions

F. Iser: Conceptualization, data curation, software, formal analysis, validation, investigation, visualization, methodology, writing–original draft, writing–review and editing. **F. Hinz:** Conceptualization, data curation, software, formal analysis, validation, investigation, visualization, methodology, writing–original draft, writing–review and editing. **D.C. Hoffmann:** Data curation, methodology, writing–review and editing. **N. Grassl:** Investigation, writing–review and editing. **C. Güngör:** Conceptualization, resources, data curation, supervision, funding acquisition, validation, investigation, methodology, writing–original draft, project administration, writing–review and editing. **J. Meyer:** Investigation, writing–review and editing. **L. Dörner:** Investigation, writing–review and editing. **L. Hofmann:** Investigation, writing–review and editing. **V. Kelbch:** Investigation, writing–review and editing. **K. Göbel:** Software, investigation, writing–review and editing. **M.A. Mahmutoglu:** Software, investigation, methodology, writing–review and editing. **P. Vollmuth:** Resources, investigation, methodology, writing–review and editing. **A. Patel:** Resources, data curation, software, methodology, writing–review and editing. **D. Nguyen:** Data curation, software, writing–review and editing. **L.D. Kaulen:** Data curation, software, formal analysis, writing–review and editing. **I. Mildenberger:** Formal analysis, investigation, writing–review and editing. **K. Sahm:** Investigation, writing–review and editing. **K. Maaß:** Investigation, methodology, writing–review and editing. **K.W. Pajtler:** Methodology, writing–review and editing. **G.M. Shankar:** Methodology, writing–review and editing. **M. Weiler:** Methodology, writing–review and editing. **B. Wildemann:** Methodology, writing–review and editing. **F. Winkler:** Investigation, writing–review and editing. **A. von Deimling:** Resources, investigation, project administration, writing–review and editing. **M. Platten:** Resources, project administration, writing–review and editing. **W. Wick:** Conceptualization, resources, supervision, funding acquisition, writing–original draft, project administration, writing–review and editing. **F. Sahm:** Conceptualization, resources, supervision, funding acquisition, validation, methodology, writing–original draft, project administration, writing–review and editing. **T. Kessler:** Conceptualization, resources, data curation, supervision, funding acquisition, validation, methodology, writing–original draft, project administration, writing–review and editing.

Acknowledgments

We thank the patients and their families for participating in the study. We also thank all doctors, nurses, and study assistants who took part in clinical care and collection of liquid biopsy samples for their contribution to this work. The work was supported by the SFB grant UNITE Glioblastoma (SFB1389 to W. Wick, F. Sahm, and T. Kessler) of the German Research Foundation (DFG) and by a grant from the Else Kröner-Fresenius-Stiftung for cfDNA sequencing (to T. Kessler). F. Sahm received funding for liquid biopsies from the Sibylle Assmus Stiftung.

Note

Supplementary data for this article are available at Clinical Cancer Research Online (http://clincancerres.aacrjournals.org/).

Received September 25, 2023; revised November 18, 2023; accepted January 29, 2024; published first January 31, 2024.

References

1. Ostrom QT, Cioffi G, Waite K, Kruchko C, Barnholtz-Sloan JS. CBTRUS statistical report: primary brain and other central nervous system tumors diagnosed in the United States in 2014–2018. Neuro Oncol 2021;23:iii1–iii105.
2. Stupp R, Mason WP, van den Bent MJ, Weller M, Fisher B, Taphoorn MJ, et al. Radiotherapy plus concomitant and adjuvant temozolomide for glioblastoma. N Engl J Med 2005;352:987–96.

3. Louis DN, Perry A, Wesseling P, Brat DJ, Cree IA, Figarella-Branger D, et al. The 2021 WHO classification of tumors of the central nervous system: a summary. Neuro Oncol 2021;23:1231–51.
4. Corcoran RB, Chabner BA. Application of cell-free DNA analysis to cancer treatment. N Engl J Med 2018;379:1754–65.
5. Wan JCM, Massie C, Garcia-Corbacho J, Mouliere F, Brenton JD, Caldas C, et al. Liquid biopsies come of age: towards implementation of circulating tumour DNA. Nat Rev Cancer 2017;17:223–38.
6. Bettegowda C, Sausen M, Leary RJ, Kinde I, Wang Y, Agrawal N, et al. Detection of circulating tumor DNA in early-and late-stage human malignancies. Sci Transl Med 2014;6:224ra24.
7. Miller AM, Shah RH, Pentsova EI, Pourmaleki M, Briggs S, Distefano N, et al. Tracking tumour evolution in glioma through liquid biopsies of cerebrospinal fluid. Nature 2019;565:654–8.
8. Cantor E, Wierzbicki K, Tarapore RS, Ravi K, Thomas C, Cartaxo R, et al. Serial H3K27M cell-free tumor DNA (cf-tDNA) tracking predicts ONC201 treatment response and progression in diffuse midline glioma. Neuro Oncol 2022;24:1366–74.
9. Miller AM, Szalontay L, Bouvier N, Hill K, Ahmad H, Rafailov J, et al. Next-generation sequencing of cerebrospinal fluid for clinical molecular diagnostics in pediatric, adolescent and young adult brain tumor patients. Neuro Oncol 2022;24:1763–72.
10. Orzan F, De Bacco F, Lazzarini E, Crisafulli G, Gasparini A, Dipasquale A, et al. Liquid biopsy of cerebrospinal fluid enables selective profiling of glioma molecular subtypes at first clinical presentation. Clin Cancer Res 2023;29:1252–66.
11. Gupta M, Burns EJ, Georgantas NZ, Thierauf J, Nayyar N, Gordon A, et al. A rapid genotyping panel for detection of primary central nervous system lymphoma. Blood 2021;138:382–6.
12. Zuccato JA, Patil V, Mansouri S, Voisin M, Chakravarthy A, Shen SY, et al. Cerebrospinal fluid methylome-based liquid biopsies for accurate malignant brain neoplasm classification. Neuro Oncol 2023;25:1452–60.
13. Afflerbach A-K, Rohrandt C, Brändl B, Sönksen M, Hench J, Frank S, et al. Classification of brain tumors by nanopore sequencing of cell-free DNA from cerebrospinal fluid. Clin Chem 2024;70:250–60.
14. Kickingereder P, Isensee F, Tursunova I, Petersen J, Neuberger U, Bonekamp D, et al. Automated quantitative tumour response assessment of MRI in neuro-oncology with artificial neural networks: a multicentre, retrospective study. Lancet Oncol 2019;20:728–40.
15. Isensee F, Jäger PF, Kohl SA, Petersen J, Maier-Hein KH. Automated design of deep learning methods for biomedical image segmentation. arXiv:190408128; 2019.
16. Isensee F, Schell M, Pflueger I, Brugnara G, Bonekamp D, Neuberger U, et al. Automated brain extraction of multisequence MRI using artificial neural networks. Hum Brain Mapp 2019;40:4952–64.
17. Katzendobler S, Do A, Weller J, Dorostkar MM, Albert NL, Forbrig R, et al. Diagnostic yield and complication rate of stereotactic biopsies in precision medicine of gliomas. Front Neurol 2022;13:822362.
18. Platten M, Bunse L, Wick A, Bunse T, Le Cornet L, Harting I, et al. A vaccine targeting mutant IDH1 in newly diagnosed glioma. Nature 2021;592:463–8.
19. Boschert T, Kromer K, Lerner T, Lindner K, Haltenhof G, Tan CL, et al. Neoepitope-specific vaccination of a patient with diffuse midline glioma targeting H3K27M induces polyclonal B and T cell responses across diverse HLA alleles. bioRxiv; 2023.
20. Mellinghoff IK, van den Bent MJ, Blumenthal DT, Touat M, Peters KB, Clarke J, et al. Vorasidenib in IDH1-or IDH2-mutant low-grade glioma. N Engl J Med 2023;389:589–601.